

SLOW LIGHT

PACS numbers: 42.50.–p; 78.67.De
DOI: 10.1070/QE2015v045n01ABEH015596

Theoretical analysis of multiple quantum-well, slow-light devices under applied external fields using a fully analytical model in fractional dimension

R. Kohandani, H. Kaatuzian

Abstract. **We report a theoretical study of optical properties of AlGaAs/GaAs multiple quantum-well (MQW), slow-light devices based on excitonic population oscillations under applied external magnetic and electric fields using an analytical model for complex dielectric constant of Wannier excitons in fractional dimension. The results are shown for quantum wells (QWs) of different width. The significant characteristics of the exciton in QWs such as exciton energy and exciton oscillator strength (EOS) can be varied by application of external magnetic and electric fields. It is found that a higher bandwidth and an appropriate slow-down factor (SDF) can be achieved by changing the QW width during the fabrication process and by applying magnetic and electric fields during device functioning, respectively. It is shown that a SDF of 10^5 is obtained at best.**

Keywords: *multiple quantum well; coherent population oscillations; magnetic and electric field; fractional dimension.*

1. Introduction

The term 'slow light' refers to the propagation of an optical signal at a very low group velocity. Recently, there has been huge interest in the physics and applications of slow light [1, 2]. Several techniques to slow down the speed of light have been demonstrated, including electromagnetically induced transparency (EIT), coherent population oscillations (CPOs), stimulated Brillouin scattering (SBS) and stimulated Raman scattering (SRS) [3–6]. Using atomic vapours at a low temperature, significant slow-down of light has been achieved by EIT [7]. Despite a considerable slow-down factor (SDF), EIT relies on a long optical decoherence time. The slow light via CPOs only needs a long relaxation time and is easier to implement as compared to EIT [1, 2, 8].

Slow light is achieved in a wide variety of media and structures. In recent years there has been great interest in the slow-light effect in semiconductor nanostructures because of thier ability to integrate and better compatibility with optical integrated circuits [9, 10]. Slow light using excitonic population oscillations in QWs and quantum dots has been successfully demonstrated at low and room temperatures [1, 2, 11].

R.Kohandani, H.Kaatuzian Photonics Research Laboratory (PRL), Department of Electrical Engineering, Amirkabir University of Technology (Tehran Polytechnic), 424 Hafez Avenue, Tehran15914, Iran; e-mail: hsnkato@aut.ac.ir

Received 24 June 2014; revision received 12 August 2014
Kvantovaya Elektronika **45** (1) 89–94 (2015)
Submitted in English

The significant characteristics of the exciton in a semiconductor with a MQW structure, including exciton oscillator strength (EOS), binding energy and exciton energy, have been widely investigated. The experimental and theoretical reports demonstrate that the properties of the exciton are dependent on QW parameters [12–14]. Also, the properties of the exciton can be changed by the application of external magnetic and electric fields [15–20]. Variation in the exciton characteristics affects the optical properties of slow-light devices. Therefore, the optical properties of slow-light devices can be tuned by changing QW parameters during the fabrication process [21, 22]. Accordingly, applying external magnetic and electric fields allows optical properties to be tuned during the device functioning [23].

2. Theory

2.1. Fully analytical model in non-integer dimension for a MQW, slow-light device based on CPOs

The group velocity of a light pulse as it propagates through a dispersive material is defined as [24]:

$$v_{\rm gr} = \frac{c}{n_{\rm gr}} = \frac{c}{n(\omega) + \omega {\rm d}n(\omega)/{\rm d}\omega}, \quad (1)$$

where $n(\omega)$ is the refractive index of the material and c is the speed of light in vacuum. A considerable reduction in the speed of light can be achieved at very large and positive ${\rm d}n/{\rm d}\omega$. The slow-light phenomenon occurs in the vicinity of material resonances, where the slope of the real part of refractive index sharply varies.

In a two-level system, if the difference frequency between the pump and the signal is within the range of the inverse carrier lifetime, coherent population beatings will be generated at this frequency. Coherent population beatings can produce a dip in the absorption spectrum, and at zero signal-pump detuning the group velocity decreases [1]. In a semiconductor nanostructure, this two-level system can be a heavy–hole (HH) exciton of QWs.

Figure 1 shows the pump-probe scheme of a MQW, slow-light device based on the CPO effect. According to the model developed in [25, 26], the refractive index of MQW structures in the vicinity of the band gap can be achieved by calculating the complex dielectric function of Wannier excitons in fractional dimension. In this model, the complex dielectric constant is calculated by solving the Schrödinger equation in a noninteger dimension and is defined as follows:

$$\varepsilon(E) = \frac{SR^{d/2-1}}{E+i\gamma}\{g_d[\xi(E+i\gamma)] + g_d[\xi(-E-i\gamma)] - 2g_d[\xi(0)]\}, \quad (2)$$

$$g_d(\xi) = 2\pi\Gamma\left(\frac{d-1}{2}+\xi\right) \times\left[\Gamma\left(\frac{d-1}{2}\right)^2\Gamma\left(1-\frac{d-1}{2}+\xi\right)\xi^{d-2}\right]^{-1} \times\left\{\cot\left[\pi\left(\frac{d-1}{2}-\xi\right)\right]-\cot[\pi(d-1)\right\}, \quad (3)$$

$$\xi(Z) = \left(\frac{R}{E_g - Z}\right)^{1/2}, \quad (4)$$

where $\Gamma(X)$ is the Euler function; S is a parameter related to the EOS; and R and E_g are the effective Rydberg constant and band gap energy, respectively. The total dielectric constant for the MQW structure, including HH and light-hole (LH) contributions, is:

$$\varepsilon(E) = 1 + \varepsilon_{\text{background}} + \varepsilon_{\text{HH}}(E) + \varepsilon_{\text{LH}}(E). \quad (5)$$

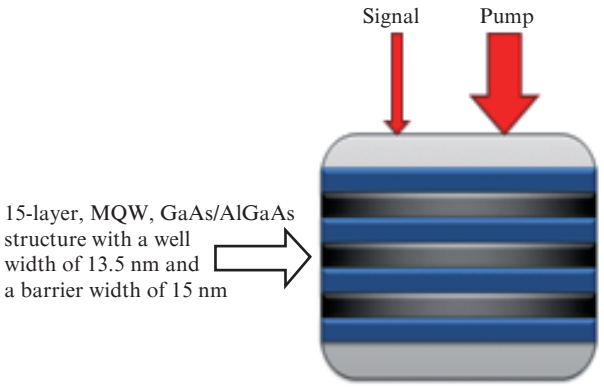

Figure 1. Schematic diagram of an $Al_{0.3}Ga_{0.7}As/GaAs$ MQW, slow-light device based on CPOs and described in [1].

For modelling an MQW, slow-light device, we consider only the HH contribution while neglecting the LH contribution. Also for slow-light purpose, the sign of dielectric function of the HH contribution is changed. This is due to the pump–signal configuration and absorption cancellation in the slow-light, CPO-based mechanism [21]. The refractive index n_s, absorption A_s and SDF R_s are defined, respectively, as follows:

$$n_s(E) = \sqrt{\varepsilon_s(E)}, \quad (6)$$

$$A_s(E) = 2\frac{\omega_s}{c}\text{Im}[n_s(E)], \quad (7)$$

$$R_s(E) = \text{Re}[n_s(E)] + \omega_s\frac{\partial\,\text{Re}[n_s(E)]}{\partial E}. \quad (8)$$

Therefore, based on this modified model and using equations (6), (7) and (8), the absorbance, real part of the refractive index and SDF of the MQW, slow-light device can be calculated, as shown in Fig. 2.

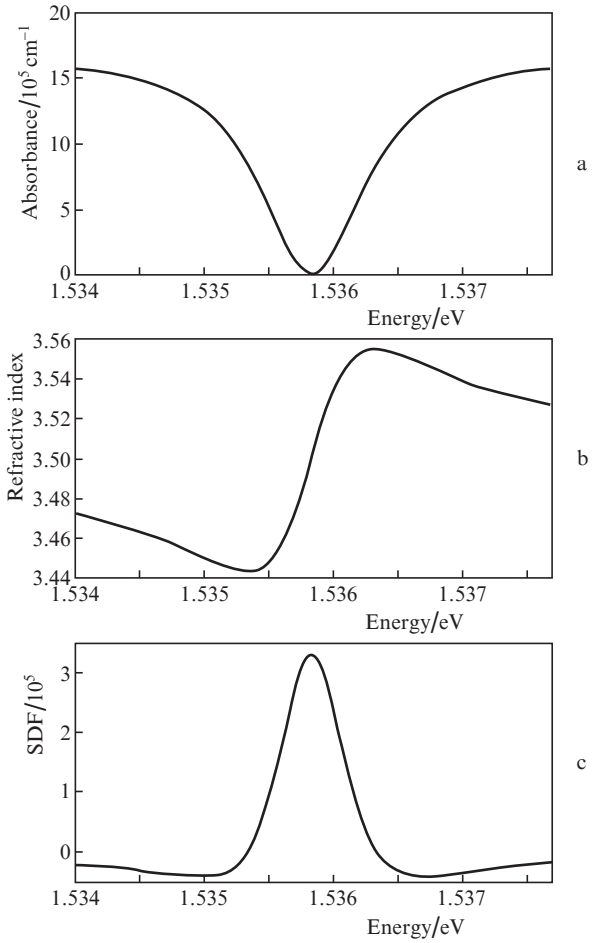

Figure 2. (a) Absorbance, (b) real part of the refractive index and (c) SDF appearing due to excitonic population oscillations as functions of energy.

The results provide good agreement with both the experiment and the theoretical model presented in [1]. The maximum value of the SDF is reached at an energy of 1.5358 eV, which corresponds to the photon energy of the pump and hence the excitonic energy. The values of the parameters which are used for these calculations can be found in [21, 25, 26].

2.2. Effects of QW width variations

Dependence of EOS on QW width. In MQW structures, the area under absorption peaks for heavy-hole excitons, is directly proportional to f/L_w, where f is the EOS quantity, and L_w is the QW width. In addition, for narrow wells, this area is inversely proportional to L_w^2 As a result, f is inversely proportional to L_w [12, 13, 21]. Figure 3 shows the dependence of EOS on QW width for the AlGaAs/GaAs MQW. It is clear that as the QW width becomes narrower, the value of EOS becomes larger. The parameters which are used for calculations are the same as in Refs [12, 13, 21].

Dependence of fractional dimension on QW width. To describe optical properties of semiconductors, which could not be analysed using well-known methods in pure two-dimensional (2D) and three-dimensional (3D) spaces, the

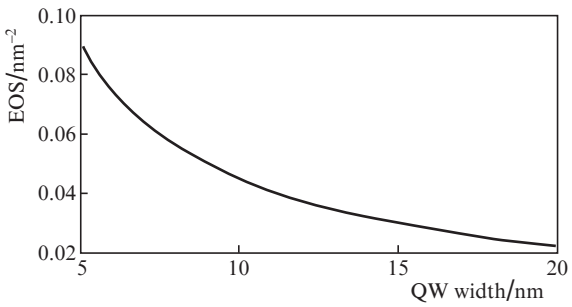

Figure 3. Dependence of the EOS on the QW width for an $Al_{0.3}Ga_{0.7}As$/GaAs MQW.

concept of the fractional dimensional space is introduced. In this approach, the anisotropic problem in a 3D space becomes isotropic in a lower fractional-dimensional space, where the value of dimension is determined by the degree of anisotropy. In QW structures, depending on the ratio of the QW width to the exciton Bohr radius, the value of the fractional dimension can vary between 2 and 3. Also, fractional dimension is related to the spatial extension k_b^{-1} of the exciton in the barriers [25–27].

The fractional dimension of a finite QW is given by [14]:

$$d = 3 - \exp\left[-\left(\frac{2}{k_b} + L_w\right)\frac{1}{2a_0^*}\right], \tag{9}$$

where a_0^* is the mean value of the three-dimensional Bohr radius.

Figure 4 shows the dependence of fractional dimension on QW width for a GaAs/AlGaAs MQW. The values of the parameters can be found in [14].

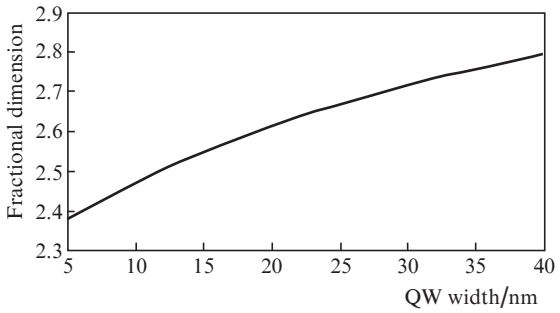

Figure 4. Dependence of the fractional dimension on the QW width for an $Al_{0.3}Ga_{0.7}As$/GaAs MQW.

2.3. Effects of an applied magnetic field on an AlGaAs/GaAs MQW

Diamagnetic shift of exciton energy levels. Consider a MQW device situated in a magnetic field, which is parallel to the growth axis of excitons. The applied magnetic field leads to an enhancement of the exciton energy levels. The value of diamagnetic shift E' for the 1s-level exciton can be obtained as follows [15]:

$$E' = \int \left(N_{1s}\cos\frac{\pi z_e}{L}\cos\frac{\pi z_h}{L}\right)^2 H' \mathrm{d}z_e \mathrm{d}z_h \mathrm{d}x\mathrm{d}y, \tag{10}$$

$$H' = \frac{e^2B^2}{8\mu_\pm e^2}(x^2 + y^2), \tag{11}$$

where μ is the reduced mass of excitons; B is the magnetic field; and x, y, z_e and z_h are the components of the coordinate vectors.

Figure 5 shows a diamagnetic shift of the ground state energy of the exciton in an AlGaAs/GaAs MQW as a function of the magnetic field calculated for $L_w = 13.5$ nm.

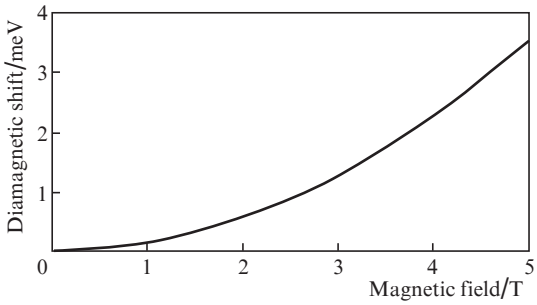

Figure 5. Dependence of the diamagnetic shift of exciton energy levels in an AlGaAs/GaAs MQW on the applied magnetic field.

Enhancement of the EOS. The oscillator strength of the exciton can be increased by application of a magnetic field. An applied magnetic field draws the electron and hole together and modifies the in-plane motion of them and thus increases the EOS [19, 20, 15]. The exciton wave function can be defined as:

$$\Psi(z_e, z_h, r) = f_e(z_e) f_h(z_h) \Psi(r), \tag{12}$$

where $f_e(z_e)$ and $f_h(z_h)$ are the confined electron and hole states in the well and $\Psi(r)$ is the in-plane exciton wave function. As the magnetic field applies to the MQW structure, $\Psi(r)$ can be calculated by solving the appropriate Hamiltonian for the exciton motion under an applied magnetic field. The oscillator strength of the exciton under an applied field is [19, 20]:

$$f \propto |\Psi(0)|^2 \left| \int f_e(z_e) f_h(z_h) \mathrm{d}z \right|^2. \tag{13}$$

The dependence of the EOS on the magnetic field is due to the effect of the diamagnetic term on Ψ [20]. Therefore, an applied magnetic field leads to an enhancement of the EOS. Figure 6 demonstrates variations in the EOS due to an applied magnetic field for an AlGaAs/GaAs MQW.

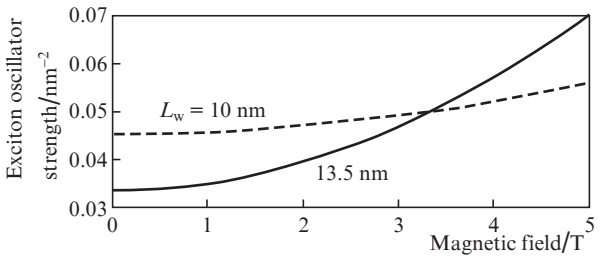

Figure 6. Dependences of the exciton oscillator strength on the magnetic field applied to an AlGaAs/GaAs MQW.

2.4. Effects of an applied electric field on an AlGaAs/GaAs MQW

Stark shift in exciton absorption. An electric field, which is applied to a MQW perpendicularly, pulls electrons and holes in opposite sides. This phenomenon leads to a reduction in energy of an electron–hole pair and a Stark shift in the exciton absorption [16–18].

Figure 7 illustrates the exciton peak shift due to an applied electric field for $L_w = 13.5$ nm. The parameters which are used for calculation are the same as in Refs [16–18].

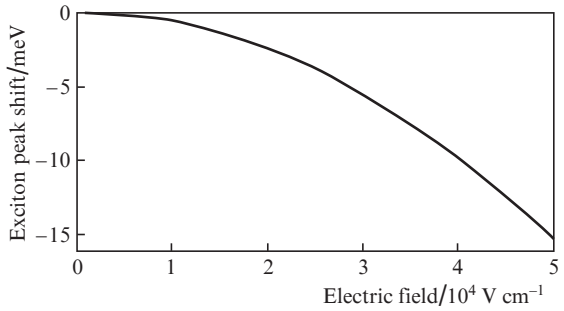

Figure 7. Dependene of the exciton peak shift on the applied electric field applied to an AlGaAs/GaAs MQW.

EOS reduction. The oscillator strength of the exciton can be decreased by applying an electric field. According to equation (13), the oscillator strength of the exciton under an applied electric field is proportional to a simple overlap integral between the conduction band and HH wave functions [17–20]. Figure 8 demonstrates the variation in the EOS due to application of an electric field for a MQW structure [17, 18].

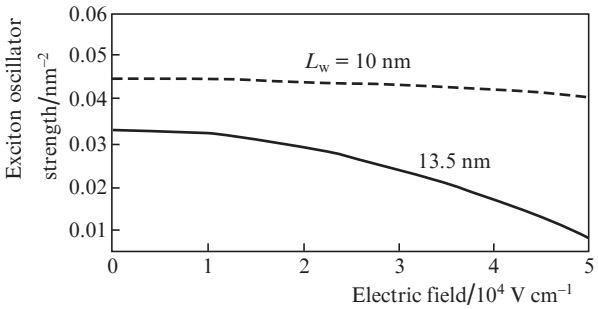

Figure 8. Dependences of the EOS on the electric field applied to an AlGaAs/GaAs MQW.

3. Results and discussion

3.1. Prefabrication tuning of a slow-light device by altering the QW width

Based on the theory presented in Section 2.2, QW width alterations have two effects on MQW properties. Changing QW width affects the value of the EOS and the value of the fractional dimension. Therefore, the optical properties of the slow-light device, such as SDF and central frequency, can be changed by altering the QW width.

Figures 9 and 10 show the real part of the refractive index and slow-down factor of a slow-light device at different values of QW widths. One can see that the central energy of the slow-light device decreases with decreasing QW width. Also, the slope of the real part of the refractive index is higher for narrower QW widths. The variation in the central energy is due to changes in the fractional dimension, and the slope of the real part of the refractive index alters because of variation in the EOS. Therefore, the optical properties of the slow-light device can be tuned by altering the QW width during the fabrication process.

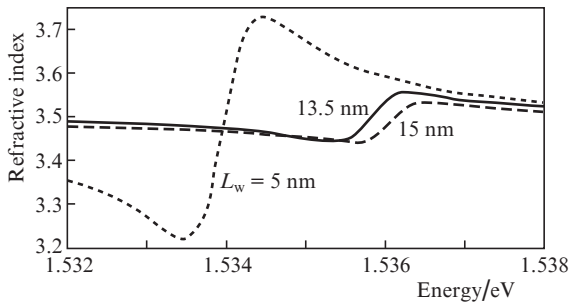

Figure 9. Dependences of the real part of the refractive index on the QW width; the solid curve shows the experimental result from [1].

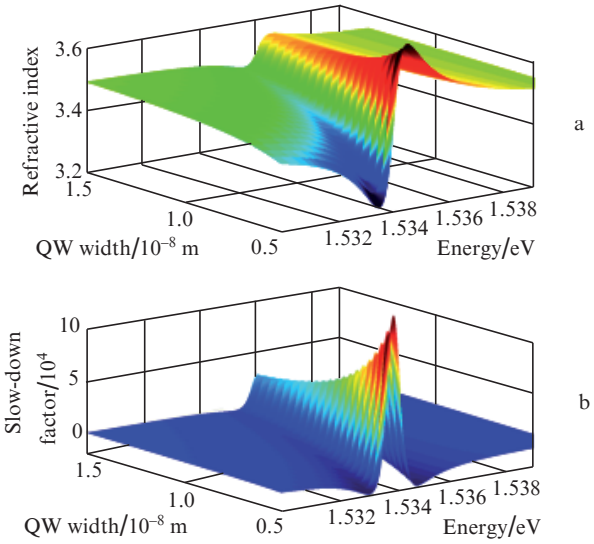

Figure 10. Dependences of (a) the real part of the refractive index and (b) the slow-down factor on the energy and QW width.

3.2. Tuning of slow-light device characteristics by applying a magnetic field

Figures 11 and 12 demonstrate the real part of the refractive index and slow-down factor for the slow-light device under an applied magnetic field. One can see that the presence of the magnetic field leads to an increase in the exciton energy and therefore to the oscillator strength of the exciton. In addition, the slope of the real part of the refractive index increases with increasing EOS.

Figure 13 shows the variations in the maximum value of the SDF as functions of QW width and applied magnetic field. One can see that the effect of the applied magnetic field

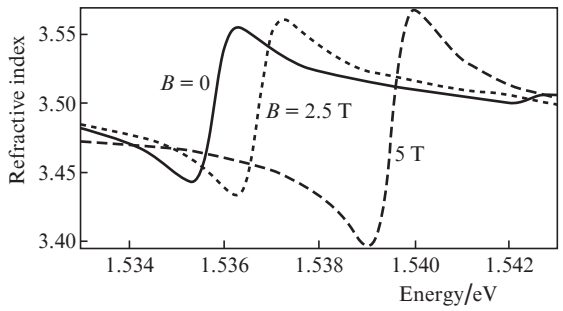

Figure 11. Dependences of the real part of the refractive index on the magnetic field; the solid curve shows the experimental result from [1].

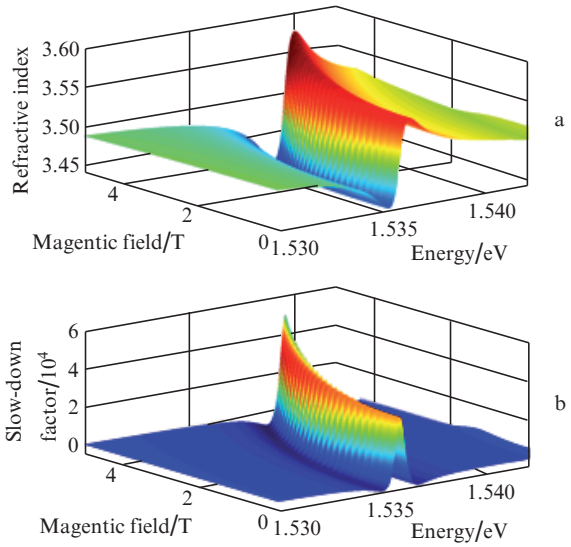

Figure 12. Dependences of (a) the real part of the refractive index and (b) the slow-down factor on the energy and applied magnetic field.

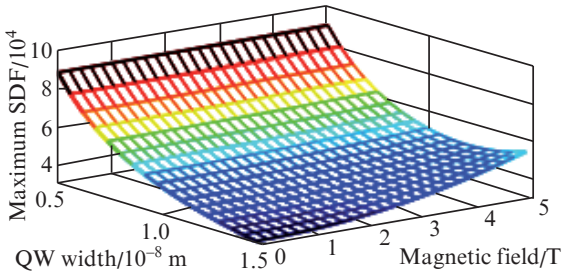

Figure 13. Dependences of the maximum value of the SDF on simultaneous alterations of the QW width and applied magnetic field.

on the maximum value of the SDF is weak for narrow wells. Also, the effective length of the QWs is constant.

3.3. Tuning of slow-light device characteristics by applying an electric field

Figure 14 shows the real part of the refractive index of the slow-light device at different applied electric fields. One can see that when the electric field is applied to the slow-light device, the exciton energy decrease and causes a down-shift in the central energy of the device. In addition, the slope of the

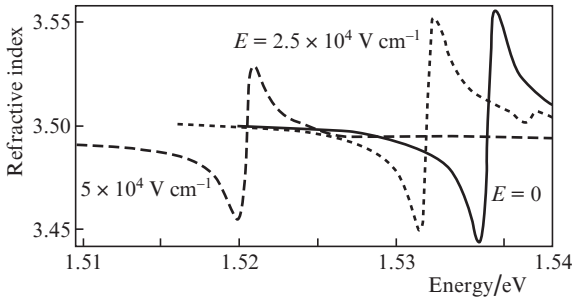

Figure 14. Dependences of the real part of the refractive index on the electric field; the solid curve shows the experimental result from [1].

real part of the refractive index decreases with decreasing EOS.

Figure 15 illustrates the real part of the refractive index and the slow down factor of the slow-light device as functions of energy and applied electric field.

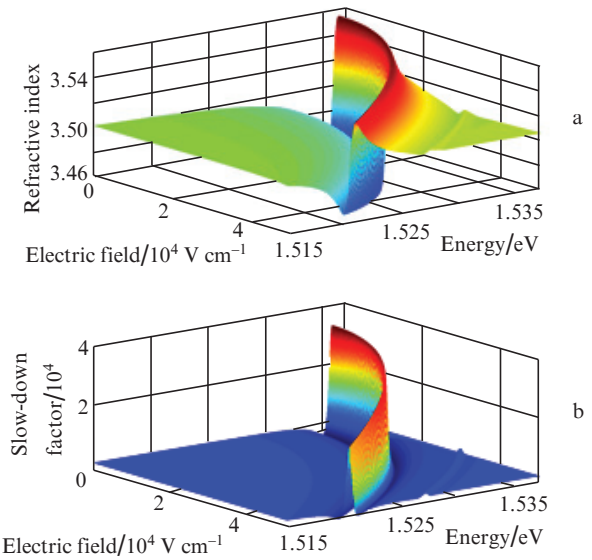

Figure 15. Dependences of (a) the real part of the refractive index and (b) the slow-down factor on the energy and applied electric field.

Figure 16 demonstrates the dependence of the maximum value of the SDF on the QW width and applied electric field. One can see that for narrow wells the effect of the applied

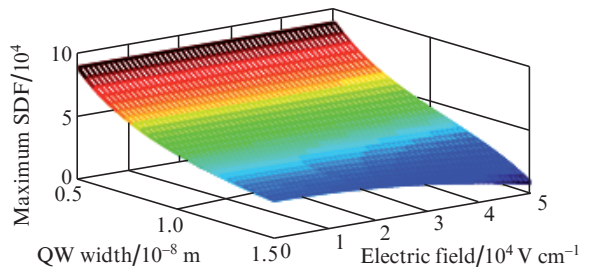

Figure 16. Dependence of the maximum value of the SDF on simultaneous alterations of the QW width and applied electric field.

electric field on the EOS is weak, because for narrow wells the right-hand side of Eqn (13) becomes very small.

3.4. Post-fabrication tuning by applying magnetic and electric fields simultaneously

An applied magnetic field affects the diamagnetic shift of the exciton energy levels and the oscillator strength of the exciton. Application of an electric field decreases the exciton energy and hence the EOS value. Figure 17 shows the variation in the central energy shift and maximum value of the SDF for the slow-light device by applying simultaneously magnetic and electric fields. One can see that an appropriate SDF and central energy can be achieved by applying magnetic and electric fields to the slow-light device after fabrication.

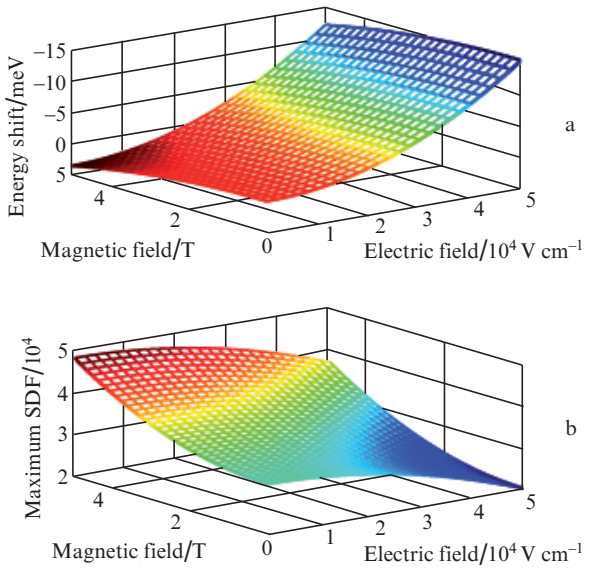

Figure 17. Dependences of (a) the central energy shift and (b) the maximum value of the SDF on the simultaneous application of the magnetic and electric fields.

4. Conclusions

In this work, we have investigated AlGaAs/GaAs multiple quantum-well, slow-light devices based on excitonic population oscillations under applied external magnetic and electric fields, using a fully analytical model in fractional dimension. The results demonstrate that both magnetic and electric fields cause alterations in the slow-down factor and central energy of the slow-light device. An applied magnetic field causes an up-shift in the central energy and leads to an enhancement of the SDF, whereas an applied electric field decreases the value of the SDF and causes a down-shift in the central energy. The slow down factor can be maximised by reducing QWs width under high magnetic fields and can be minimised by increasing QWs width under strong electric fields. These results can be used for tuning optical properties of slow-light devices and can be applicable for all-optical switches, optical modulators and variable optical delays.

References

1. Chang S.W., Chuang S.L., Ku P.C., Chang-Hasnian C.J., Palinginis P., Wang H. *Phys. Rev. B*, **70**, 235333 (2004).
2. Chang S.W., Chuang S.L. *Phys. Rev. B*, **72**, 235330 (2005).
3. Kaatuzian H. *Photonics* (Teheran: AKU, 2009) Vol. 2.
4. Bigelow M.S., Lepeshkin N.N., Boyd R.W. *Science*, **301** (5630), 200 (2003).
5. Okawachi Y., Bigelow M.S., Sharping J.E., Zhu Z., Schweinsberg A., Gauthier D.J., Boyd R.W., Gaeta A.L. *Phys. Rev. Lett*., **94** (15), 153902 (2005).
6. Sharping J.E., Okawachi Y., Gaeta A.L. *Opt. Express*, **13** (16), 6092 (2005).
7. Hau L.V., Harris S.E., Dutton Z., Behroozi C.H. *Nature*, **397** (6720), 594 (1999).
8. Ku P.C., Sedgwick F., Chang-Hasnain C.J., Palinginis P., Li T., Wang H., Chang S.W., Chuang S.L. *Opt. Lett*., **29**, 2291 (2004).
9. Ma S.M., Xu H., Ham B.S. *Opt. Express*, **17**, 18364 (2009).
10. Yan W., Wang T., Li X.M., Jin Y.J. *Appl. Phys. B*, **108**, 515 (2012).
11. Palinginis P., Sedgwick F., Crankshaw S., Moewe M., Chang-Hasnain C.J. *Opt. Express*, **13**, 9909 (2005).
12. Zhang B., Kano S.S., Shiraki Y. *Phys. Rev. B*, **50** (11), 7499 (1994).
13. Andreani L.C., Pasquarello A. *Phys. Rev. B*, **42** (14), 8928 (1990).
14. Mathieu H., Lefebvre P., Christol P. *Phys. Rev. B*, **46** (7), 4092 (1992).
15. Bugajski M., Kuszko W., Regifiski K. *Sol. State Commun*., **60** (8), 669 (1986).
16. Miller D.A.B., Chemla D.S., Damen T.C., Gossard A.C., Wiegmann W., Wood T.H., Burrus C.A. *Phys. Rev. Lett*., **53**, 2173 (1984).
17. Sanders G.D., Bajaj K.K. *Phys. Rev. B*, **35** (5), 2308 (1987).
18. Yu P.W., Sanders G.D., Evans K.R., Reynolds D.C., Baja K.K., Stutz C.E., Jones R.L. *Phys. Rev. B*, **40** (5), 3151 (1989).
19. Bauer G.E.W., Ando T. *Phys. Rev. B*, **38** (9), 6015 (1988).
20. Whittaker D.M., Fisher T.A., Afshar A.M., Skolnick M.S., Kinsler P., Roberts J.S., Hill G., Pate M.A. *Il Nuovo Cimento D*, **17**, 1781 (1995).
21. Kaatuzian H., Shokri Kojori H., Zandi A., Ataei M. *Opt. Quantum Electron*., **45**, 947 (2013).
22. Kaatuzian H., Shokri Kojori H., Zandi A., Kohandani R. *Opt. Photon. J*., **3**, 298 (2013).
23. Kohandani R., Zandi A., Kaatuzian H. *Appl. Opt*., **53**, 1228 (2014).
24. Khurgin J.B., Tucker R.S. *Slow Light Science and Applications* (London: CRC Press, 2009).
25. Tanguy C., Lefebvre P., Mathieu H., Elliott R.J. *J. Appl. Phys*., **82**, 798 (1997).
26. Marquezini M.V., Tignon J., Hasche T., Chemla D.S. *Appl. Phys. Lett*., **73**, 2313 (1998).
27. He X. *Phys. Rev. B*, **43** (3), 2063 (1991).